Carbon 129 (2018) 159–167

Contents lists available at ScienceDirect

Carbon

journal homepage: www.elsevier.com/locate/carbon

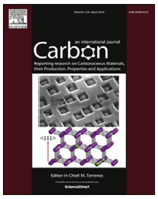

Revealing the formation mechanism of ultrahard nanotwinned diamond from onion carbon

Hu Tang [a, b], Xiaohong Yuan [a], Pengfei Yu [a], Qingyang Hu [b, c], Mingzhi Wang [a, *], Yansun Yao [d, **], Lailei Wu [a], Qin Zou [a, ***], Yujiao Ke [a], Yucheng Zhao [a], Lei Wang [e], Xiaopu Li [a], Wenge Yang [f], Huiyang Gou [b, ****], Ho-kwang Mao [f, h], Wendy L. Mao [c]

[a] *State Key Laboratory of Metastable Materials Science and Technology, Yanshan University, Qinhuangdao 066004, China*
[b] *Center for High Pressure Science and Technology Advanced Research, Beijing 100094, China*
[c] *Geological Sciences, Stanford University, Stanford, USA*
[d] *Department of Physics and Engineering Physics, University of Saskatchewan, Saskatoon, SK, S7N 5E2, Canada*
[e] *Qinhuangdao Institute of Technology, Qinhuangdao, Hebei 066100, China*
[f] *Center for High Pressure Science and Technology Advanced Research, Shanghai 201203, China*
[h] *Geophysical Laboratory, Carnegie Institution of Washington, Washington, DC 20015, USA*

HPSTAR
502-2018

ARTICLE INFO

Article history:
Received 1 August 2017
Received in revised form
30 November 2017
Accepted 8 December 2017
Available online 8 December 2017

ABSTRACT

Controlled nanotwinning is an effective way to enhance the mechanical properties of materials. Recent discovery of nanotwinned diamond converted from carbon nano-onions with high-density defects reveals that the presence of nanotwinned structures can increase the hardness of the product to exceed that of natural diamond by a surprisingly large margin. To understand the mechanism of nanotwinning, the microscopic transformation pathway from carbon nano-onions to nanotwinned diamond was investigated in the present study. We carried out a direct high-pressure high-temperature synthesis of nanotwinned diamond from onion carbon without high-density defects. The obtained nanotwinned diamond possesses an exceptionally high Vickers hardness of 215 GPa at 4.9 N. The transformation path was analyzed using aberration-corrected transmission electron microscopy (TEM) which suggests a martensitic process strongly influenced by the pressure-temperature conditions. Specifically, the appearance of {111} nanotwinned structure and stacking faults was determined by the characteristics of the onion shells, while the accumulation of the stress due to the sliding of the shells cause the crystal to re-align along the shear direction. These findings not only clarify the direct transformation mechanism from onion-like precursors to nanotwinned diamond, but also have broad implications for further exploration of new materials with exceptional properties.

1. Introduction

Diamond is the hardest material currently known. Extensive efforts have been devoted to finding new materials with the hardness exceeding that of diamond. In theory, cubic C_3N_4 and lonsdaleite (hexagonal diamond) have been predicted to have mechanical properties superior to those of diamond [1–3]. Although new superhard carbon phase can be synthesized under high-pressure within DAC (diamond-anvil cell) [4–6]. Experimental realizations of new materials in bulk (other than pure carbon) that are harder than diamond have not been successful. One approach to enhance the material strength is by manipulating its grain size, known as the Hall-Petch relationship [7–9]. The strength of a polycrystalline material should increase, up to a limit, with decreasing grain size. This can be understood in terms of the dislocations accumulated at the grain boundaries, such that when the grain size is reduced, the nucleation and motion of dislocations are suppressed, thereby strengthening the material. Nano-polycrystalline diamond (NPD) with a grain size of 10–30 nm has

---

* Corresponding author.
** Corresponding author.
*** Corresponding author.
**** Corresponding author.

E-mail addresses: wangmingzhi_future@163.com (M. Wang), yansun.yao@usask.ca (Y. Yao), zq@ysu.edu.cn (Q. Zou), huiyang.gou@gmail.com (H. Gou).

https://doi.org/10.1016/j.carbon.2017.12.027
0008-6223/

been synthesized from direct conversion of graphite at high pressure and high temperature (HPHT), and exhibits an exceptionally high hardness of 110–140 GPa [7]. NPD with smaller grain sizes (5–10 nm) can be prepared using amorphous carbon, C_{60} or glassy carbon precursors [10]. The mechanical properties of the latter, however, decrease dramatically with the grain size. This reversed Hall-Petch effect indicates that other factors, for example poorly sintered grain boundaries or sliding motions at the boundaries should become significant once the grain size is reduced to below a critical length.

Nanotwinning is known as a highly effective approach for strengthening structural materials and impeding the degradation of mechanical properties [11–16]. In strong covalent materials like diamond, however, nanotwinning was thought to be extremely challenging due to the large stacking fault energy (SFE). Recently a major breakthrough was realized when nanotwinned cubic-BN (*nt-c*-BN) and diamond (*nt*-diamond) were successfully synthesized from onion-like nanoparticle precursors under HPHT conditions [17,18]. The products that were obtained demonstrate significantly improved mechanical properties compared to their bulk counterparts. In particular, the *nt*-diamond exhibits an ultrahigh Vickers hardness of ~200 GPa, which is about twice that of natural diamond (~100 GPa), and also much greater than the maximum hardness obtained in NPD (~140 GPa) [7]. The application of nano-onion precursors with high-density defects has been regarded as a key ingredient for the successful synthesis of ultrahard carbon materials.

Carbon nano-onions are multi-shelled nanoparticles consisting of concentric graphitic shells. Ideally, the center shell is a C_{60} molecule and the number of atoms in outer shells increases by $N = 60n^2$ fashion where n is the index of the shell [19–21]. A typical inter-shell distance in carbon nano-onions is close to the intersheet distance of graphite, which is 0.334 nm. The number of shells in the carbon nano-onions can be altered which leads to different physical and chemical properties that may find use in various applications [22–24], and considerable progress has been made toward synthesizing onion carbon and manipulating the particle size and morphologies [25–29]. The *nt*-diamond was synthesized using carbon nano-onions as precursors (20–50 nm in size) prepared from black carbon through an impinging-streams technology. The precursors contain a high concentration of puckered layers and stacking faults, which were thought to be the key for the nucleation of *nt*-diamond [18,30].

To date, the formation mechanism from carbon nano-onion precursors to *nt*-diamond has not been fully addressed [18,30–32]. It is generally understood that the twin boundaries, *i.e.*, crystalline interfaces with minor lattice mismatch, are thermodynamically more stable than conventional grain boundaries, and this is the reason for the increased hardness in *nt*-diamond compared to NPD. Understanding the microscopic origin of the twin boundaries, and the formation of such from onion-like precursors, are therefore critically important and can provide guidance to the production of *nt*-diamond at a larger scale. In this study, the onion carbon without high-density defects were prepared by annealing detonated nanodiamond, and subsequently used for HPHT synthesis of *nt*-diamond. Nanotwinned structures were characterized in the products and the nucleation mechanism was analyzed using multiple experimental and theoretical methods. The structural transformation from onion carbon to *nt*-diamond is shown to be a martensitic process, in which the high-density defects may not be necessary for the formation of nanotwinning, but they do play a role in lowering the onset of the transition pressure. The hardness of the synthesized *nt*-diamond was measured and analyzed along with the microstructure of the products.

2. Materials and methods

2.1. Synthesis of carbon onion nanoparticles and high-pressure experiments

The nano-diamond starting material with an average grain size of about 5 nm was purchased from Heyuan Zhonglian Nano Technology Co. Ltd, China (Fig. S1). Surface impurities, mainly functional groups of −OH or C=O, were eliminated in the annealing process. Carbon onion nanoparticles were prepared by annealing the high-disperse detonated nano-diamond at temperature of 1500 °C for 30 min in a ZT-25-20 type vacuum carbon tube furnace (~0.1 Pa). A heating rate of 10 °C/min was employed during the annealing process. Subsequently, the annealed onion carbon nanoparticles were placed in an *h*-BN capsule and treated at HPHT with a 10-MN double-stage multi-anvil system, in which the standard COMPRES 10/5 (10–15 GPa) and 8/3 (15–25 GPa) assemblies consisting of a spinel ($MgAl_2O_4$) + MgO octahedron with a Re heater and a $LaCrO_3$ thermal insulator were used [17]. The assembly schematic is presented in Fig. S2. Temperatures were measured with W–Re (type C) thermocouples. Pressures were previously calibrated at room temperature using the diagnostic changes in the electrical resistances of ZnTe (9.6 and 12.0 GPa), ZnS (15.5 GPa), GaAs (18.3 GPa) and GaP (23.0 GPa) because of the semiconductor–metal phase transitions at high pressures. In situ synchrotron X-ray ($\lambda = 0.4066$ Å) diffraction experiment was carried out by using DAC at station 16ID-B of High-Pressure Collaborative Access Team (HPCAT), Advanced Photon Source (APS), Argonne National Laboratory (ANL). The compression and decompression experiments were conducted at room-temperature. We used pieces of ruby as pressure calibrants, with measurements uncertainties up to 2.0 GPa.

2.2. Characterization of onion carbon and HPHT samples

An x-ray powder diffractometer (D8 Discover) with Cu Kα radiation ($\lambda = 0.15406$ nm) was employed for the phase characterization of the annealed onion carbon and the recovered HPHT samples. More structural characteristics of onion carbon and HPHT samples were investigated by aberration-corrected transmission electron microscopy (TEM), high-resolution TEM (HRTEM) and electron energy loss spectroscopy (EELS), which were performed with a FEI Titan-G2 type electron microscope operated at 300 kV. Raman spectra were recorded on a Renishaw Raman microscope with an excitation wavelength of 532 nm.

2.3. Vickers hardness measurements of HPHT samples

A micro-Vickers hardness tester (FM-700, Future-Tech, Japan) was used to evaluate the hardness of recovered samples. Hardness values were measured using a Vickers diamond indenter with a load of 4.9 N and holding time of 10 s. H_v was determined from $H_v = 1854.4F/L^2$, where F (N) is the applied load and L (μm) is the arithmetic mean of the two diagonals of the Vickers indentation.

2.4. Electronic structure and molecular dynamics simulations

Behavior of carbon materials at HPHT conditions and formation of twin boundaries in cubic diamond were simulated using molecular dynamics methods in isothermal-isobaric (NPT) ensembles with Langevin dynamics. The calculation employed Perdew–Burke–Ernzerhof (PBE) functional and projector augmented plane-wave (PAW) potentials implemented in the Vienna Ab Initio Simulation Package (VASP) program. A kinetic energy cut-off of 400 eV was used for the plane-wave basis set. Various simulation cells containing 144 and 288 carbon atoms were used at different *P*-*T* conditions. The time step used in the simulation was 2 fs and the self-consistency on the total energy was chosen to be 1 × 10^{-5} eV.

3. Results and discussion

Carbon onion nanoparticles were prepared by annealing the detonated nano-diamond, without high-density defects (Fig. S3). The products were subsequently compressed and heated to synthesize *nt*-diamond. Fig. 1*a* shows the *x*-ray diffraction (XRD) patterns of the sample recovered from 10 GPa and from two temperatures, 1600 °C and 1800 °C. The XRD pattern at 1600 °C contains Bragg reflections from cubic diamond in addition to onion carbon precursor. The presence of cubic diamond here (Fig. 1*c* and *f*) is due to the residual diamond cores in the precursors (Fig. S3*e*), which are potentially the nucleation sites for crystal growth (Fig. S4) [33]. At 1600 °C, the majority of the sample still maintains the shelled structure with large distortions (Fig. 1*e*). The Raman spectrum obtained at this temperature contains a singular peak at 1556 cm^{-1} which could be identified as *D* modes of disordered carbon [34] structures on the inner shells (Fig. 1*b*). At 1800 °C, the structural changes become noticeably more significant in the sample (Fig. 1*f-h*). Both the XRD pattern (Fig. 1*a*) and Raman spectrum (Fig. 1*b*) reveal the appearance of defective graphite (*D*, *G* and *D′* Raman modes at 1348 cm^{-1}, 1580 cm^{-1} and 1618 cm^{-1}, respectively [35]). The onion-like nanoparticles lose their integrity with the shells flattened to become the (002) planes of the graphite (Fig. 1*h*). The growth of graphite in onion-carbon matrix clearly depends strongly on the temperature (Fig. S4*e-g*).

When the temperature was held at 1800 °C and the pressure was increased to above 15 GPa, the recovered samples become transparent (Fig. 2*a* and *d*). The XRD patterns reveal that the

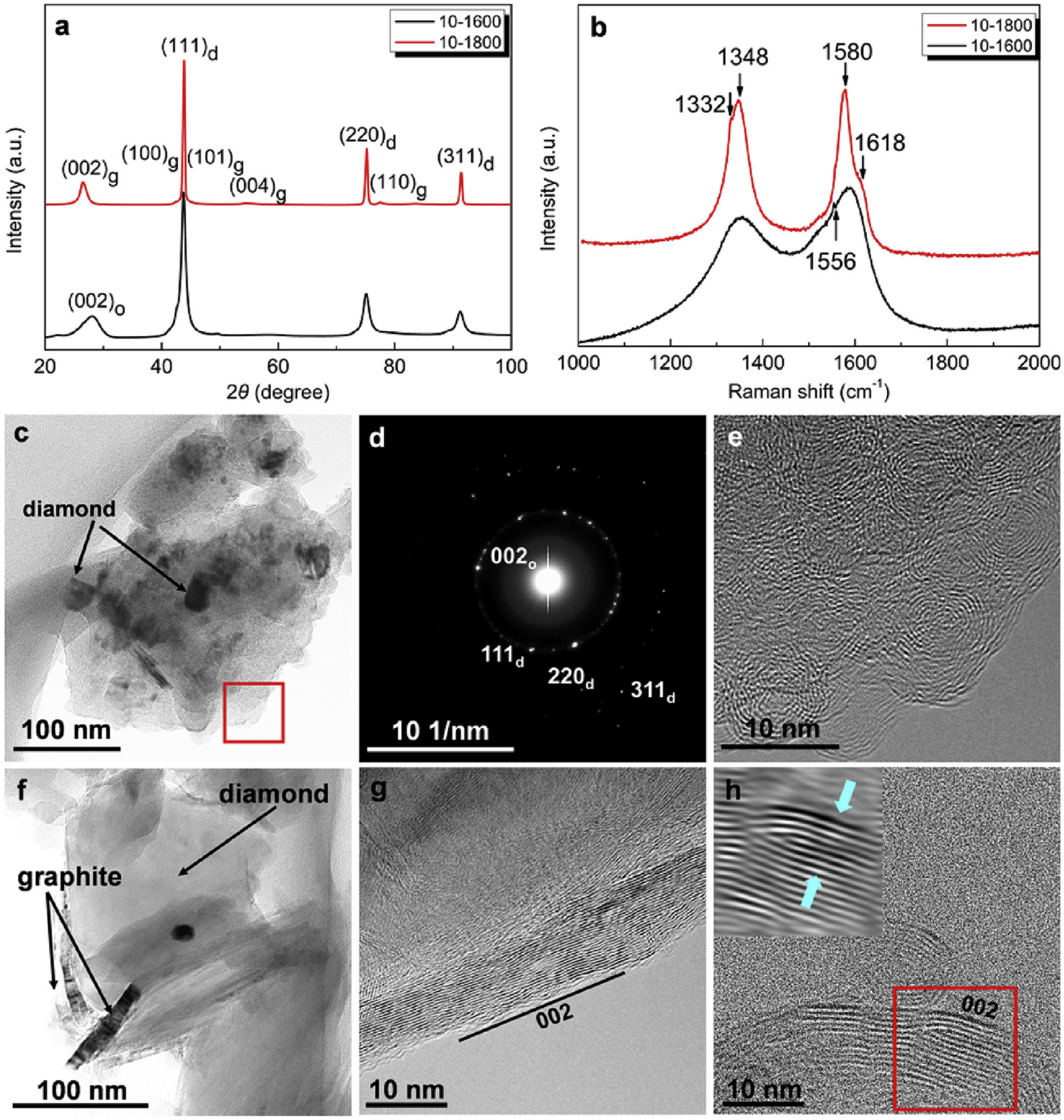

Fig. 1. a,b) XRD patterns and Raman spectra of the recovered samples from the annealed onion carbon at 10 GPa. Pressure (in GPa) and temperature (in °C) conditions are indicated by a pair of numbers in the legend. c,d) TEM image and electron diffraction (SAED) patterns in an selected area of the sample recovered at 10 GPa and 1600 °C. e) HRTEM image of the selected area marked by the red box in c. f-h) TEM image and HRTEM images of the sample recovered at 10 GPa and 1800 °C. Inverse fast Fourier transform (IFFT) image is inserted in h marked with the red box. (A colour version of this figure can be viewed online.)

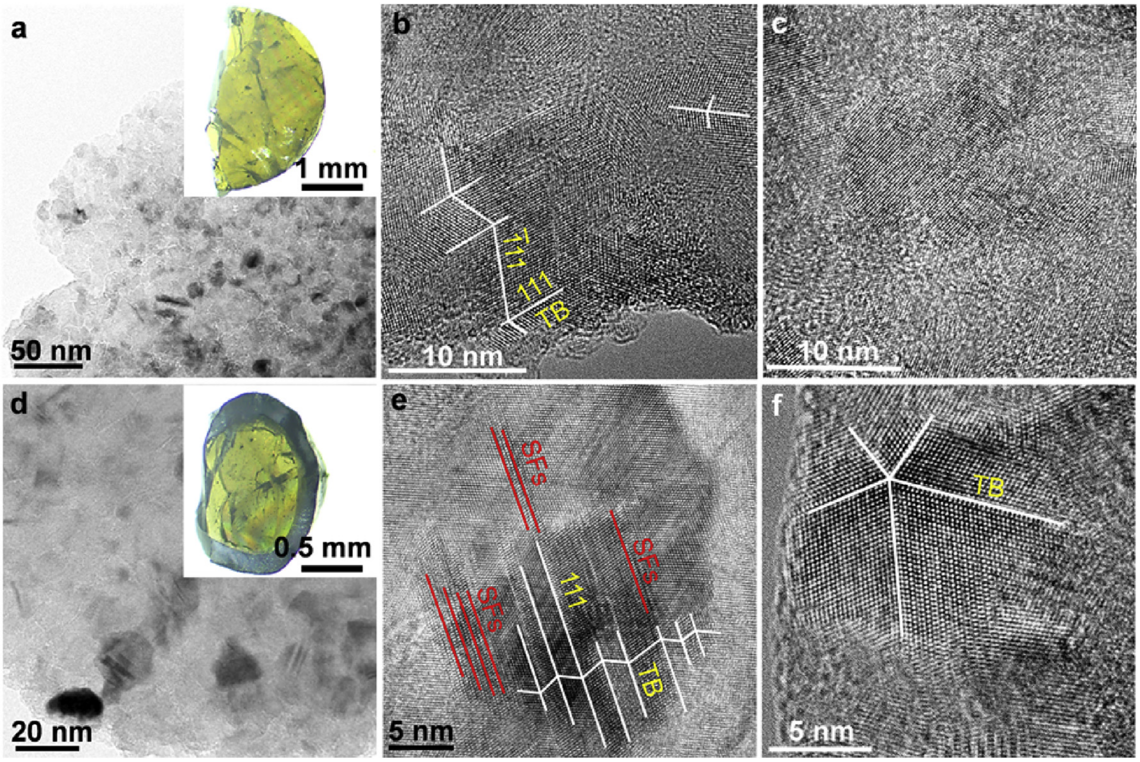

Fig. 2. a-c) TEM and HRTEM images of the sample synthesized at 15 GPa and 1800 °C. d-f) TEM and HRTEM images of samples synthesized at 25 GPa and 1800 °C. (A colour version of this figure can be viewed online.)

samples consist primarily of cubic diamond, but with no graphite or onion carbon (Fig. S5). At 20 GPa, small stacking faults, which could be {111} nanotwins of diamond, appeared in the sample (Fig. S6*a*). Upon compression to 25 GPa, high-density lamellar nanotwins and stacking faults become prominent in the recovered samples (Fig. 2*e* and Fig. S6*c*-*f*). Most intriguingly, the recovered sample shows a five-fold twinned structure in diamond (Fig. 2*f*). When the treatment temperature is lowered to 1600 °C at 25 GPa, the transformation to diamond is incomplete. As shown in Fig. 3a, distorted graphitic structures still exist along with the (002) lattice fringes of onion carbon in the recovered samples. Raman spectra obtained at different pressures and 1600 °C all show the *D* and *G* graphitic modes (Fig. 3*e*). The diamond T_{2g} mode (~1332 cm^{-1}) overlaps with the graphitic *D* mode and therefore is barely seen. Upon increasing the pressure, the *D* and *G* modes shift to lower frequencies. The weak Raman peak at 1556 cm^{-1} presents in all samples recovered at 10 GPa, 15 and 20 GPa, but disappears at 25 GPa (Figs. 1b and 3c) [34]. When the temperature is increased to 1800 °C, a very broad Raman band (1300 cm^{-1} to 1650 cm^{-1}) develops in the spectra for the samples synthesized above 15 GPa, which is very similar to the spectra previously observed in other pressurized samples synthesized from black carbon or quasi-amorphous soot precursors at similar HPHT conditions [36]. This band could be due to the residual sp^2 carbon as shown in Figs. 3*c* and S7, which is further verified by TEM-EELS analysis. As shown in Fig. 3*f*, the major peaks of the carbon *K*-edge located at 290 eV, 297 eV and 303 eV arise from the transitions from 1*s* core level to σ* band ($1s \rightarrow \sigma^*$ transition) [37,38]. The extremely weak peak at 284 eV corresponds to the $1s \rightarrow \pi^*$ transition, indicating the presence of sp^2-bonded carbon atoms.

Grain size distributions in the recovered samples were obtained from TEM observations (Fig. 4*a* and *b*). At 15 GPa and 1800 °C, the average grain size is 9.9 nm, which agrees well with the estimate from the Debye-Scherrer measurement of the XRD pattern (Table 1). With further compression to 25 GPa at the same temperature, the grain size increases to an average of 12.8 nm (Fig. 4*b*). This value is much larger than the estimate obtained from the XRD pattern, with the inconsistency likely arising from the presence of a high-concentration of nanotwins and stacking faults (Fig. 2*e*), for which the Debye-Scherrer measurement provides a poor estimate. Mechanical testing shows that the sample recovered at 25 GPa and 1800 °C has an exceptionally high Vickers hardness of 215 GPa at 4.9 N (Fig. 4*c*). Yet, the measured hardness is strongly affected by the residual sp^2 carbon between the grain boundaries, where several weak points with the Vickers hardness of 150–170 GPa are found (Fig. S8).

Generally, increasing the external pressure tends to reduce the diffusivity of atoms, which restricts the growth of the grains [8,9]. The larger average grain size obtained at 25 GPa therefore suggests that the transition from onion carbon precursor to diamond is likely a diffusionless process (martensitic transformation), similar to the graphite-to-diamond transition in bulk [39,40]. The HRTEM image (Fig. 5a) reveals that the newly formed diamond (111) planes in the sample are almost parallel to the (002) planes of the residual onion carbon, suggesting that the former is formed directly from the latter. In addition, we also observed some orthogonal lattice fringes in the samples (see Fig. 5*b*,*c*), which was previously identified as the (100) and (002) planes of hexagonal diamond (lonsdaleite) by Kulnitskiy et al. [41] Hexagonal diamond has pure sp^3 bonding like cubic diamond but with a different stacking sequence (ABAB). Previous theoretical and experimental studies suggested that cubic and hexagonal diamonds can be formed by the buckling of the basal planes of graphite with particular stacking sequences under pressure. Furthermore, based on theoretical reports the compression of hexagonal graphite with the stacking sequence (ABAB) preferentially results in hexagonal diamond instead of cubic diamond [36,39–45]. However, experimental results support that cubic

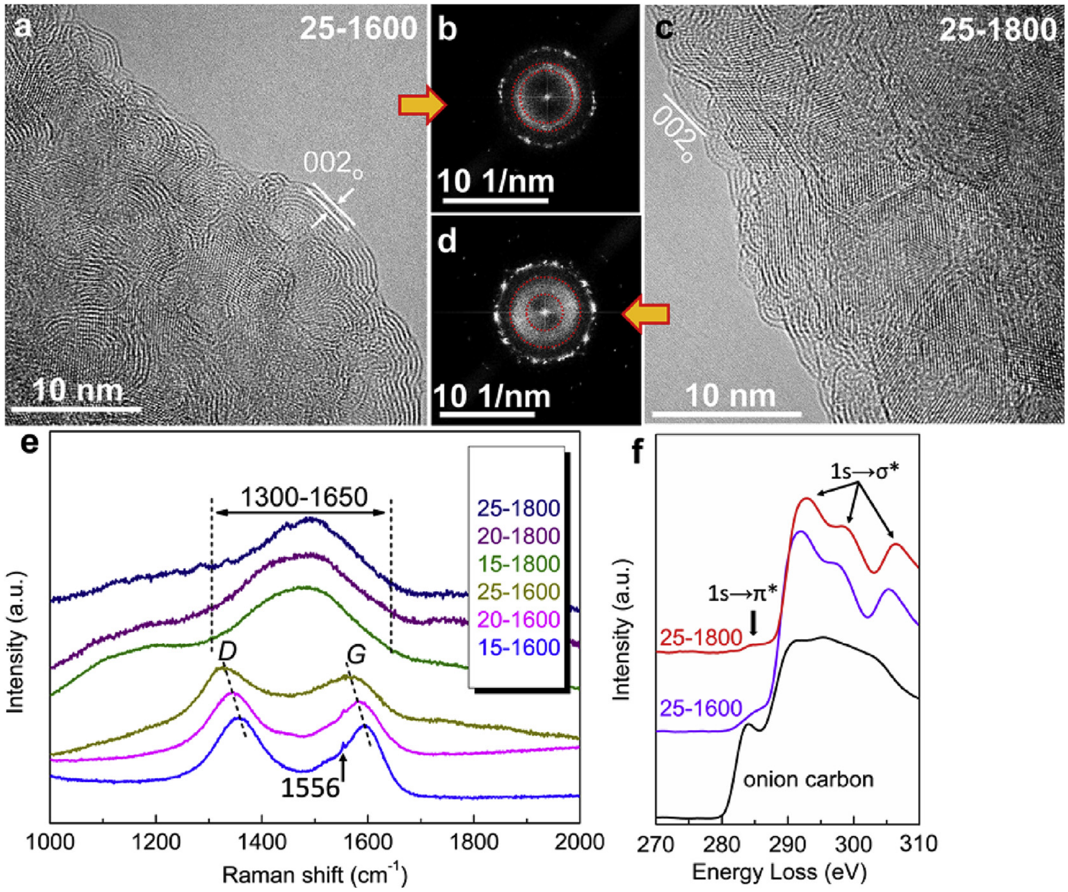

Fig. 3. HRTEM images and SAED patterns of the samples recovered at 25 GPa and at 1600 °C (a,b) and 1800 °C (c,d). e) Raman spectra of the samples recovered above 15 GPa and temperatures of 1600–1800 °C. f) EELS spectra of the samples recovered at 25 GPa and temperatures of 1600–1800 °C in comparison with the spectrum of onion carbon. (A colour version of this figure can be viewed online.)

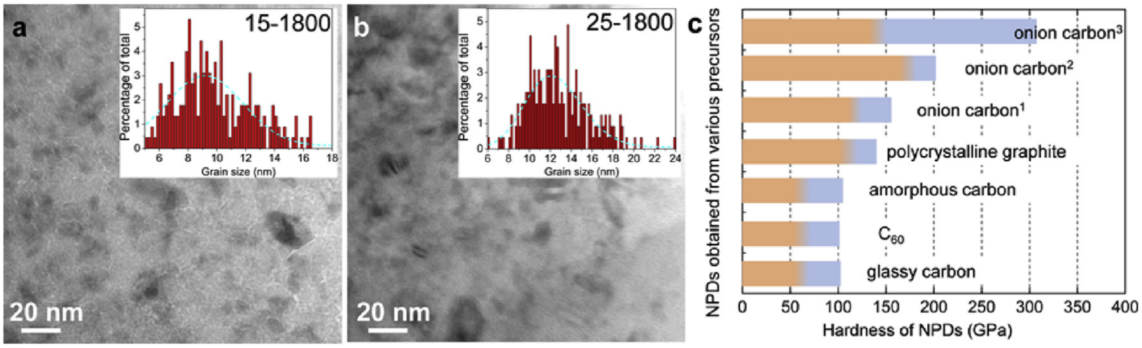

Fig. 4. TEM images and size distributions of the grains for the samples recovered at a) 15 GPa and 1800 °C, and b) 25 GPa and 1800 °C, respectively. c) The Vickers hardness of NPDs synthesized from various carbon precursors.[7,10] Superscripts differentiate three types of onion carbon precursors fabricated from different approaches. (1) Onion carbon with diamond cores produced by annealing nano-diamond at low temperature,[33] (2) Onion carbon with high-density stacking faults made from black carbon powders through an impinging-streams technology,[18] and (3) onion carbon without high-density defects produced by annealing nano-diamond at higher temperatures (present study). (A colour version of this figure can be viewed online.)

diamond is formed from polycrystalline hexagonal graphite at HPHT [7,36]. Based on recent TEM evidence, Németh et al. reinterpreted the hexagonal diamond phase as defective cubic diamond with stacking faults and twins [46,47]. Along this line, the orthogonal lattice fringes (Fig. 5c) is consistent with 90° rotation twins of cubic diamond [47]. In brief, cubic diamond cannot be directly formed from hexagonal graphite because of mismatched basal planes. Following the thermodynamic selectivity, the mismatched basal planes are shifted at high temperatures and rearranged to an ABC stacking sequence (so called 'rhombohedral graphite'). The 'chair' buckling of the planes in rhombohedral graphite leads to the formation of cubic diamond [40].

Our results suggest that the sliding of the (002) planes likewise occurs in onion carbon when it transforms into diamond following a martensitic process. A schematic diagram for the microscopic transformation paths are presented in Fig. 5*e*. Twinned cubic diamonds are formed by the rearrangements of the (002) planes, which were disordered into an ABCCBA sequence, followed by

Table 1
Full width at half maximum (FWHM) (°) and grain size (nm) derived from the XRD patterns (Fig. S3) measured for the samples synthesized at different HPHT conditions. The average grain sizes were calculated using the Scherrer equation.

NO.	*P* (GPa)	*T* (°C)	2*θ* (°)	*h k l*	FWHM (°)	Grain size (nm)
1	15	1800	43.8	111	0.78	10.9
			75.2	220	1.01	9.9
			91.4	311	1.15	9.8
2	25	1800	43.9	111	1.06	8.5
			75.2	220	1.60	6.2
			91.6	311	1.97	5.7

buckling of the planes where a sp^2 to sp^3 transition takes place. To understand the transition path, we examined the evolution of the structure of the carbon onion precursor in a cold compression up to 30 GPa. As shown in Fig. 6*a*, the Bragg peak for the (100) reflection in the sample is almost unaffected through the entire compression indicating little structural change within the planes. In contrast, the (002) reflection peak moves to higher 2-theta and keeps broadening as the applied pressure increases, and almost disappears above 22 GPa. This observation suggests that, while the inter-planer spaces are reduced as expected (Fig. 6*b*), the stacking of the (002) planes are also becoming flawed and completely disordered as the pressure increases.

The microscopic path connecting a set of sequentially disordered graphitic planes to a twinned ABC stacking was examined using *ab initio* energy calculation (Fig. 6*c*). The theoretical model was constructed using a continuous unit cell with 18 graphitic layers. At the beginning of the path, the layers are stacked randomly. At the end, the layers were ordered in ABC sequencing with two twin boundaries, which represents a ~2 nm separation between the twin boundaries. The result shows that such a plane shifting is energetically favorable, and even more so at high pressures (Fig. 6*c*). This is understandable since at high pressure the layers are brought closer together which favors direct interactions between atoms in adjacent layers at the onset of the formation of sp^3 bonding. The transition from twinned ABC graphite to twinned diamond is almost instantaneous once the compression is sufficient, as shown by the molecular dynamics simulation (Fig. 6*e*). Such a transition is expected to release a large amount of energy with an appreciable volume drop. From our experiments, the lattice ordering is facilitated by high temperature, which drives the disordered graphitic sheets to rhombohedral graphite (ABC stacking) for the formation of cubic diamond (Fig. 6*d*).

A similar diffusionless transition mechanism has been suggested for describing the bulk graphite to diamond transformation. The fundamental difference here is the formation of high-density {111} nanotwins and stacking faults (in Fig. 2*e*). A partial nanotwinned structure was also observed in the direct conversion of polycrystalline graphite into NPD under pressure, which was attributed to the suppression of the temperature-induced ordering of the (002) planes by pressure [7,48]. For onion carbon, the sliding motion of the (002) planes is limited by its confined morphology. Ideally, the concentric shells of onion carbon are closed and uniformly stressed. Sliding motions between the shells would induce additional stress, causing the C—C bonds to elongate or shorten. Under high pressure, the shell structures are deformed, and flattened to disordered graphitic layers. Mutual sliding between these layers causes the accumulation of stress. The formation of the twinned boundaries is a response to the accumulated stress, which

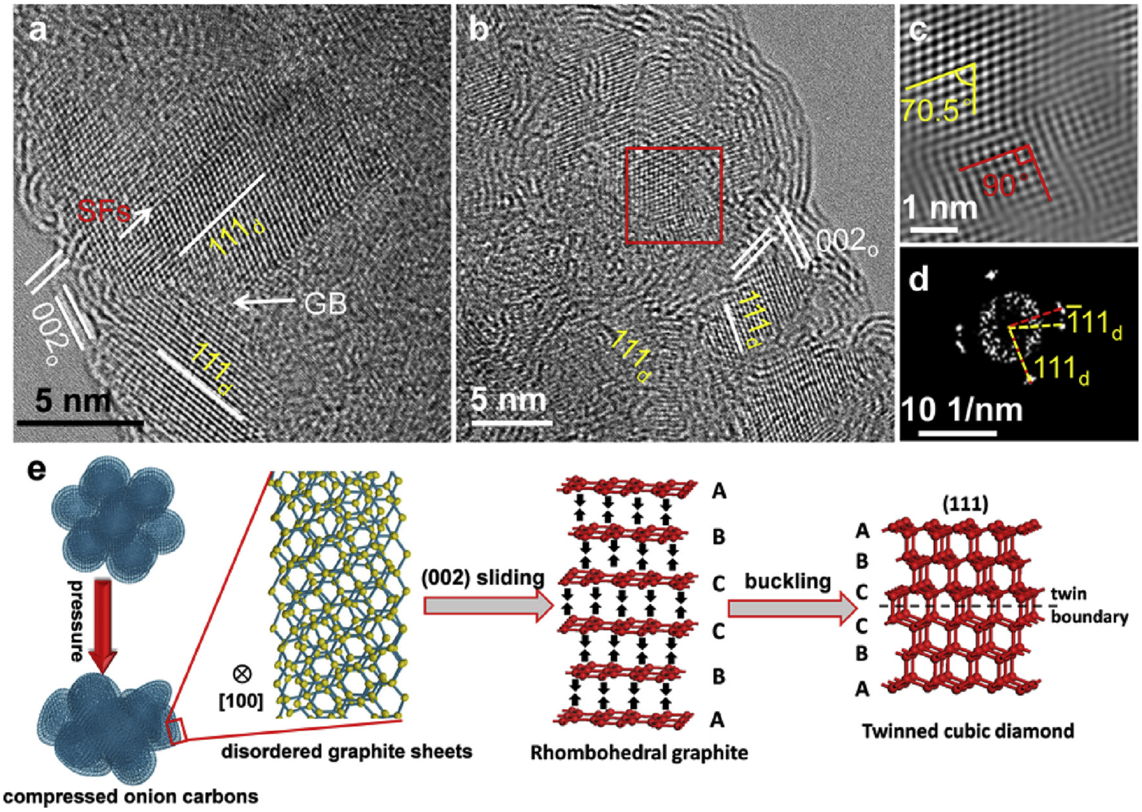

Fig. 5. a) HRTEM image of the sample recovered at 25 GPa and 1800 °C showing the formation of cubic diamond (111) planes from parallel onion carbon (002) planes. b) Cubic diamond coexisting with hexagonal diamond with a coherent boundary. c,d) IFFT image corresponding to the red box marked in b and the FFT pattern. e) Schematic diagram of transformation from onion carbon to nanotwinned cubic diamond via a martensitic process at HPHT. (A colour version of this figure can be viewed online.)

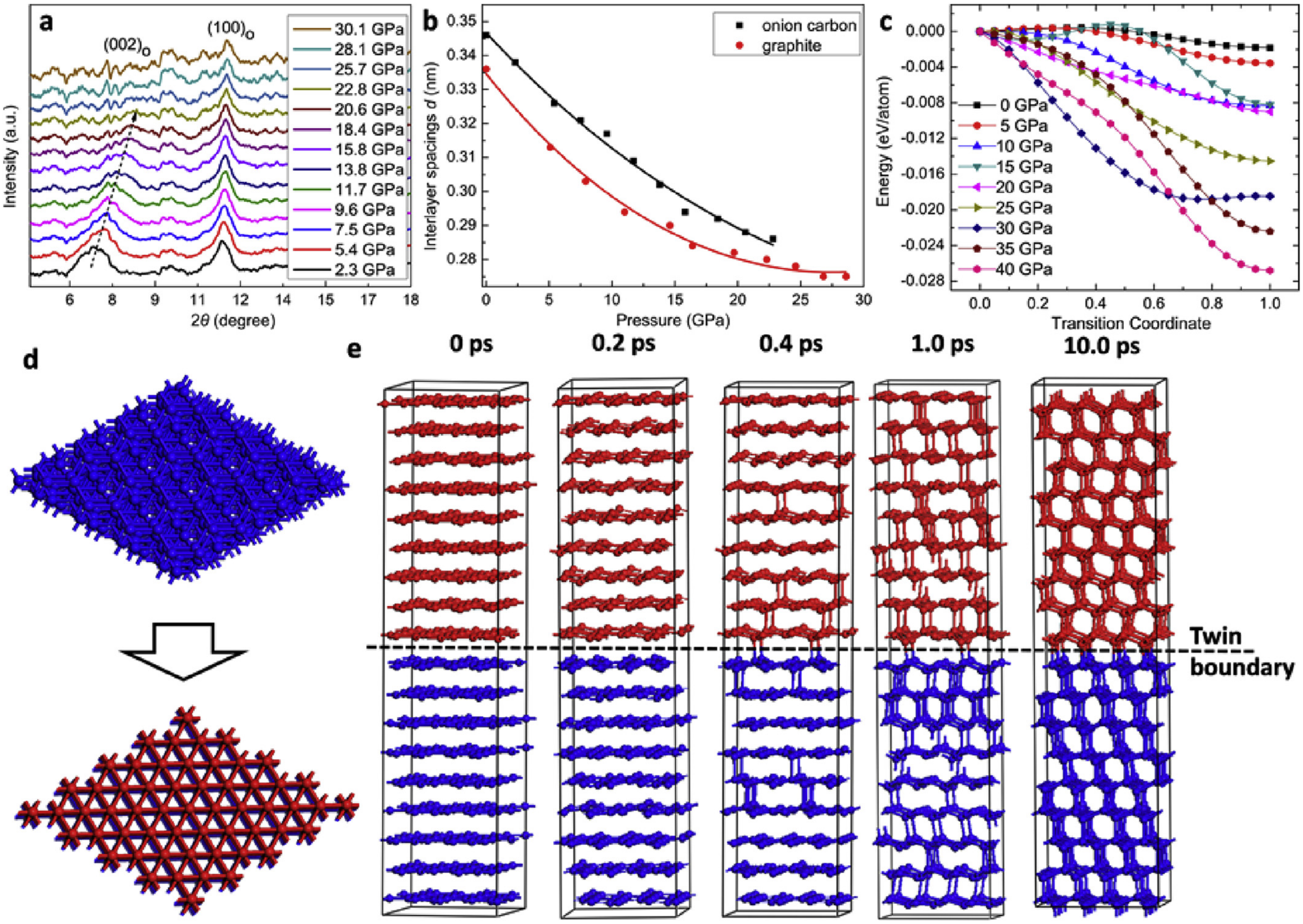

Fig. 6. a) *In-situ* XRD patterns of onion carbon obtained under different pressures at room temperature. b) Comparison of interlayer spacing for onion carbon (obtained from XRD in (a)) and graphite under pressure. c) Calculated energy changes from sequentially disordered graphite to ordered graphite with ABC stacking sequence intercepted by a twinned boundary in every 9 layers. d) View along c-axis of the disordered and ordered graphite structures. e) Evolution of the ordered graphite structure in c) to twinned cubic diamond at 30 GPa and 1800 °C simulated by molecular dynamics. The structure is over compressed to accelerate the phase transition. Atoms located on the opposite sides of the twin boundary are distinguished by colors. (A colour version of this figure can be viewed online.)

aligns the crystal along the shear direction. The twinned rhombohedral graphite (ABCCBA stacking) is formed from disordered graphitic sheets. The ‘chair’ buckling of these sheets leads to the formation of twinned cubic diamond (ABCCBA stacking) (Fig. 5*e*).

The formation of a high-concentration of {111} nanotwins and stacking faults is a consequence of the accumulated stress release in the martensitic transformation from onion carbon to diamond, which is dictated by the intrinsic structure of onion carbon. Furthermore, the applied external pressure can strongly affect the onset of nanotwinning. When the carbon onion is compressed, the inter-layer spacing reduces as the applied pressure increases. Comparison of the inter-layer spacing changes in carbon onion and graphite under pressure (Fig. 6*b*) shows that the former is less compressible, which implies that the formation of diamond should occur at a higher pressure if onion carbon precursor is used. Our results show that the high-concentration of nanotwins appears in the recovered samples above 25 GPa (Fig. 2*e*). Below 25 GPa, the shell structures of onion carbon were destroyed and the precursors transformed to either distorted graphitic sheets (Fig. 1) or diamond, where the nanotwinning is minor (Fig. 2*a*–*c*). The previously reported synthesis of *nt*-diamond at lower pressures, *i.e.*, 18–20 GPa, could be attributed to the presence of the high-concentrations of defects in the precursors, such as puckered layers and stacking faults [18], which are absent in the precursors used here. Thus, this suggests that a high-concentration of defects may not be a necessary condition for the nucleation and growth of *nt*-diamond, but they help to reduce the critical pressure for the transition. Nanotwinned morphology has also been formed at HPHT using other precursors for example black carbon with structural similarity to onion carbon [36]. Based on our findings, a variety of graphite-like carbons with multilayer continuous carbon shells are expected to be promising precursors for the synthesis of *nt*-diamond.

4. Conclusion

In summary, we report a new synthesis of nanotwinned diamond under HPHT conditions using onion carbon without high-density defects. The structural transformation behavior of onion carbon was investigated in varying *P-T* conditions. We found that without high-density defects, onion carbon preferentially transforms to distorted graphite or diamond with slight twinning at lower pressures (10–20 GPa), as opposed to the nanotwinned diamond observed in the case of synthesis using precursors with a high-concentration of defects. At higher pressure above 25 GPa, onion carbon directly transforms to nanotwinned diamond with ultrahigh hardness. Based on our experimental and theoretical results, we suggest that the phase transformation from onion carbon precursor to nanotwinned diamond is a martensitic process, in which the formation of high-concentration {111} twins and stacking faults is dictated by the characteristics of the shell structures. The relative (002) sliding motions within the onion-like structures are restricted which induce an accumulation of stress along the shear direction. The release of the stress re-aligns the C–C bonds at the boundary and leads to the formation of {111} twinned structures. This result suggests that the presence of a high-concentration of defects in the precursors is not a necessary condition for the formation of nano-twinned diamond, but they could bring down the pressure for this to occur. The present study provides critical insights into the synthesis of nano-twinned diamond and expands the fundamental understanding of structural transformation of graphite-like carbon under HPHT conditions, which may provide guidance for future synthesis of ultrahard materials with nanotwinned morphology.

Acknowledgements

This work is supported by First Batch of Young Talent Support Plan in Hebei Province, Natural Science Foundation of Hebei Province of China (E2015203232), Special Financial Grant from the China Postdoctoral Science Foundation (2015T80895), Natural Science Foundation of Hebei Province of China (E2016203425), Key Projects of Scientific and Technological Research in Hebei Province (ZD2015018), and Natural Sciences and Engineering Research Council of Canada (NSERC). H. G. thanks the financial supports of National Natural Science Foundation of China under Grants No. 51201148 and U1530402, Thousand Youth Talents Plan. Computing resources were provided by the University of Saskatchewan, WestGrid, and Compute Canada. We acknowledge Y. Meng for beamline technical support. XRD measurements were performed at sector 16ID-B, HPCAT, APS, ANL. HPCAT operations are supported by the DOE-NNSA under award number DE-NA0001974 and by the DOE-BES under award number DE-FG02-99ER45775, with partial instrumentation funding by the NSF. Use of the Advanced Photon Source was supported by the U. S. Department of Energy, Office of Science, Office of Basic Energy Sciences, under Contract No. DE-AC02-06CH11357.

Appendix A. Supplementary data

Supplementary data related to this article can be found at https://doi.org/10.1016/j.carbon.2017.12.027.

References

[1] D.M. Teter, R.J. Hemley, Low-compressibility carbon nitrides, Science 271 (5245) (1996) 53–55.
[2] C. FRONDEL, U.B. MARVIN, Lonsdaleite, a hexagonal polymorph of diamond, Nature 214 (5088) (1967) 587–589.
[3] Z. Pan, H. Sun, Y. Zhang, C. Chen, Harder than diamond: superior indentation strength of wurtzite bn and lonsdaleite, Phys. Rev. Lett. 102 (5) (2009), 055503.
[4] M. Popov, V. Mordkovich, S. Perfilov, A. Kirichenko, B. Kulnitskiy, I. Perezhogin, et al., Synthesis of ultrahard fullerite with a catalytic 3D polymerization reaction of C_{60}, Carbon 76 (9) (2014) 250–256.
[5] W.L. Mao, H.K. Mao, P.J. Eng, T.P. Trainor, M. Newville, et al., Bonding changes in compressed superhard graphite, Science 302 (5644) (2003) 425–427.
[6] L. Wang, B. Liu, H. Li, W. Yang, Y. Ding, S.V. Sinogeikin, et al., Long-range ordered carbon clusters: a crystalline material with amorphous building blocks, Science 337 (6096) (2012) 825–828.
[7] T. Irifune, A. Kurio, S. Sakamoto, T. Inoue, H. Sumiya, Materials: ultrahard polycrystalline diamond from graphite, Nature 421 (6923) (2003) 599–600.
[8] V.L. Solozhenko, O.O. Kurakevych, Y. Le Godec, Creation of nanostuctures by extreme conditions: high-pressure synthesis of ultrahard nanocrystalline cubic boron nitride, Adv. Mater. 24 (12) (2012) 1540–1544.
[9] T. Irifune, K. Kawakami, T. Arimoto, H. Ohfuji, T. Kunimoto, T. Shinmei, Pressure-induced nano-crystallization of silicate garnets from glass, Nat. Commun. 7 (2016) 13753.
[10] H. Sumiya, T. Irifune, Hardness and deformation microstructures of nano-polycrystalline diamonds synthesized from various carbons under high pressure and high temperature, J. Mater. Res. 22 (8) (2007) 2345–2351.
[11] K. Lu, L. Lu, S. Suresh, Strengthening materials by engineering coherent internal boundaries at the nanoscale, Science 324 (5925) (2009) 349–352.
[12] J. Wang, F. Sansoz, C. Deng, G. Xu, G. Han, S.X. Mao, Strong Hall–Petch type behavior in the elastic strain limit of nanotwinned gold nanowires, Nano Lett. 15 (6) (2015) 3865–3870.
[13] J. Cai, S. Shekhar, J. Wang, M. Ravi Shankar, Nanotwinned microstructures from low stacking fault energy brass by high-rate severe plastic deformation, Scr. Mater. 60 (8) (2009) 599–602.
[14] Q. Yu, Z.W. Shan, J. Li, X. Huang, L. Xiao, J. Sun, et al., Strong crystal size effect on deformation twinning, Nature 463 (7279) (2010) 335–338.
[15] J. Wang, Z. Zeng, C.R. Weinberger, Z. Zhang, T. Zhu, S.X. Mao, In situ atomic-scale observation of twinning dominated deformation in nanoscale body-centred cubic tungsten, Nat. Mater. 14 (6) (2015) 594–600.
[16] B. Li, H. Sun, C. Chen, Extreme mechanics of probing the ultimate strength of nanotwinned diamond, Phys. Rev. Lett. 117 (11) (2016) 116103.
[17] Y. Tian, B. Xu, D. Yu, Y. Ma, Y. Wang, Y. Jiang, et al., Ultrahard nanotwinned cubic boron nitride, Nature 493 (7432) (2013) 385–388.
[18] Q. Huang, D. Yu, B. Xu, W. Hu, Y. Ma, Y. Wang, et al., Nanotwinned diamond with unprecedented hardness and stability, Nature 510 (7504) (2014) 250–253.
[19] S.J. Iijima, Cryst. Direct observation of the tetrahedral bonding in graphitized carbon black by high resolution electron microscopy, Growth 50 (3) (1980) 675–683.
[20] D. Ugarte, Curling and closure of graphitic networks under electron-beam irradiation, Nature 359 (6397) (1992) 707–709.
[21] H.W. Kroto, Carbon onions introduce new flavour to fullerence studies, Nature 359 (6397) (1992) 670–671.
[22] D. Pech, M. Brunet, H. Durou, P. Huang, V. Mochalin, Y. Gogotsi, et al., Ultrahigh-power micrometre-sized supercapacitors based on onion-like carbon, Nat. Nanotechnol. 5 (9) (2010) 651–654.
[23] J.K. McDonough, A.I. Frolov, V. Presser, J. Niu, C.H. Miller, T. Ubieto, et al., Influence of the structure of carbon onions on their electrochemical performance in supercapacitor electrodes, Carbon 50 (9) (2012) 3298–3309.
[24] M. Zeiger, N. Jäckel, V. Mochalin, V. Presser, Review: carbon onions for electrochemical energy storage, J. Mater. Chem. A 4 (2015) 3172–3196.
[25] V.L. Kuznetsov, A.L. Chuvilin, Y.V. Butenko, I.Y. Mal'kov, V.M. Titov, Onion-like carbon from ultra-disperse diamond, Chem. Phys. Lett. 222 (4) (1994) 343–348.
[26] Q. Zou, M. Wang, B. Lv, Y. Li, H. Yu, L. Zou, et al., Fabrication of onion-like carbon from nanodiamond by annealing, Wuhan. Univ. Technol. Sci. Ed. 24 (6) (2009) 935–939.
[27] J.H. Los, N. Pineau, G. Chevrot, G. Vignoles, J.M. Leyssale, Formation of multiwall fullerenes from nanodiamonds studied by atomistic simulations, Phys. Rev. B 80 (15) (2009) 155420.
[28] M. Choucair, J.A. Stride, The gram-scale synthesis of carbon onions, Carbon 50 (3) (2012) 1109–1115.
[29] T. Seto, A. Inoue, H. Higashi, Y. Otani, M. Kohno, M. Hirasawa, Phase transition and restructuring of carbon nanoparticles induced by aerosol laser irradiation, Carbon 70 (1) (2014) 224–232.
[30] Q. Tao, X. Wei, M. Lian, H. Wang, X. Wang, S. Dong, et al., Nanotwinned diamond synthesized from multicore carbon onion, Carbon 120 (2017) 405–410.
[31] G.A. Dubitsky, N.R. Serebryanaya, V.D. Blank, E.A. Skryleva, B.A. Kulnitsky, B.N. Mavrin, et al., Effect of high pressures and temperatures on carbon nano-onion structures: comparison with C_{60}, Russ. Chem. Bull. 60 (3) (2011) 413–418.
[32] W. Zhang, M. Yao, X. Fan, S. Zhao, S. Chen, C. Gong, et al., Pressure-induced transformations of onion-like carbon nanospheres up to 48 GPa, Chem. Phys. 142 (3) (2015), 34702.
[33] H. Tang, M. Wang, D. He, Q. Zou, Y. Ke, Y. Zhao, Synthesis of nano-polycrystalline diamond in proximity to industrial conditions, Carbon 108 (2016) 1–6.
[34] D.S. Knight, W.B. White, Characterization of diamond films by Raman spectroscopy, J. Mater. Res. 4 (2) (1989) 385–393.
[35] R.J. Nemanich, S.A. Solin, First- and second-order Raman scattering from finite-size crystals of graphite, Phys. Rev. B 20 (2) (1979) 392–401.
[36] C.L. Guillou, F. Brunet, T. Irifune, H. Ohfuji, J.N. Rouzaud, Nanodiamond nucleation below 2273 K at 15 GPa from carbons with different structural organizations, Carbon 45 (3) (2007) 636–648.
[37] S. Tomita, M. Fujii, S. Hayashi, K. Yamamoto, Electron energy-loss spectroscopy of carbon onions, Chem. Phys. Lett. 305 (3) (1999) 225–229.
[38] J. Xiao, J.L. Li, P. Liu, G.W. Yang, A new phase transformation path from nanodiamond to new-diamond via an intermediate carbon onion, Nanoscale 6 (24) (2014) 15098–15106.
[39] S. Scandolo, M. Bernasconi, G.L. Chiarotti, P. Focher, E. Tosatti, Pressure-induced transformation path of graphite to diamond, Phys. Rev. Lett. 74 (20) (1995) 4015–4018.
[40] R.Z. Khaliullin, H. Eshet, T.D. Kühne, J. Behler, M. Parrinello, Nucleation mechanism for the direct graphite-to-diamond phase transition, Nat. Mater. 10 (9) (2011) 693–697.
[41] B. Kulnitskiy, I. Perezhogin, G. Dubitsky, V. Blank, Polytypes and twins in the diamond–Lonsdaleite system formed by high-pressure and high-temperature

treatment of graphite, Acta Crystallogr. Sect. B Struct. Sci. Cryst. Eng. Mater. 69 (5) (2013) 474–479.

[42] T. Yagi, W. Utsumi, M. Yamakata, T. Kikegawa, O. Shimomura, High-pressure in situ x-ray-diffraction study of the phase transformation from graphite to hexagonal diamond at room temperature, Phys. Rev. B 46 (10) (1992) 6031–6039.

[43] F. Isobe, H. Ohfuji, H. Sumiya, T. Irifune, Nanolayered diamond sintered compact obtained by direct conversion from highly oriented graphite under high pressure and high temperature, J. Nanomater. (2013) 15.

[44] L.A.J. Garvie, P. Németh, P.R. Buseck, Transformation of graphite to diamond via a topotactic mechanism, Am. Mineral. 99 (2–3) (2014) 531–538.

[45] Y.P. Xie, X.J. Zhang, Z.P. Liu, Graphite to diamond: origin for kinetics selectivity, J. Am. Chem. Soc. 139 (7) (2017) 2545–2548.

[46] P. Németh, L.A.J. Garvie, T. Aoki, N. Dubrovinskaia, L. Dubrovinsky, P.R. Buseck, Lonsdaleite is faulted and twinned cubic diamond and does not exist as a discrete material, Nat. Commun. 5 (2014) 5447.

[47] P. Németh, L.A.J. Garvie, P.R. Buseck, Twinning of cubic diamond explains reported nanodiamond polymorphs, Sci. Rep. 5 (2015) 18381.

[48] K. Tanigaki, H. Ogi, H. Sumiya, K. Kusakabe, N. Nakamura, M. Hirao, et al., Observation of higher stiffness in nanopolycrystal diamond than monocrystal diamond, Nat. Commun. 4 (2013) 2343.